JTTEE5 11:129-133

Study on Plasma Sprayed Boron Carbide Coating

Yi Zeng, Soo W. Lee, and Chuanxian Ding

(Submitted 19 September 2000)

The microstructure, phase composition, and mechanical properties of boron carbide coatings formed by atmospheric plasma spraying (APS) are studied in the present work. The boron carbide coating with high microhardness and low porosity could be produced by APS. The decomposition of boron carbide powder during the plasma spray process would result in the formation of the B_xC phase and an increase of the carbon phase, which is confirmed by transmission electron microscopy, x-ray photoelectron spectroscopy, and x-ray diffraction results.

Keywords boron carbide coating, mechanical property, microstructure, phase composition

1. Introduction

Boron carbide coatings possess excellent resistance to thermal shock and good stability with respect to fusion plasma erosion, and are becoming increasingly significant in nuclear fusion plants.[1] Furthermore, the high hardness and modulus of B_4C is expected to lead to spinoffs with respect to coatings for components that are subjected to wear.[2] However, its high melting point (2450 °C), high specific heat, and high melting enthalpy make B_4C a very difficult material to melt by means of spraying.[3] Research on B_4C coatings has focused on the spray process and its influence on coating properties, such as outgassing performance, and laser testing.[4-6] However, the properties of plasma spray coatings depend strongly on their microstructure and phase composition. There has been relatively little investigation into the microstructure by using transmission electron microscopy (TEM) since the production of dense B_4C coatings is difficult. The object of the present work was to investigate the microstructure of plasma-sprayed boron carbide coatings and the relationship between the microstructure and its properties with respect to successfully produced dense B_4C coatings.

2. Experimental Procedures

The specimens were produced by atmospheric plasma spraying (APS-Plasma Technik System, Plasma Technik, Wohlen, Switzerland) on stainless steel substrates that were sandblasted with corundum. A commercial boron carbide powder (Superhard Materials Co., Mudanjiang, China) containing 0.2 wt.% O and 0.4 wt.% Fe was used as the feedstock. The specimen geometry was 30 × 40 × 2 mm and the coating thickness was 200 μm.

Yi Zeng and **Soo W. Lee,** Sun Moon University, Department of Material Engineering, Asan City, South Korea; and **Chuanxian Ding,** Shanghai Institute of Ceramics, Chinese Academy of Science, Shanghai, Peoples Republic of China. Contact e-mail: zyidq_2000@yahoo.com.

X-ray powder diffraction (XRD) analysis with CuKα radiation determined the phases present in the as-sprayed coating. Scanning electron microscopy (SEM) and TEM were used to observe the as-sprayed coating structure.

Thin-foil samples were prepared to allow TEM examination of the coating using methods that have been described elsewhere.[7] TEM examination was carried out (model 2000STEM, JEOL, Tokyo, Japan) at an accelerating voltage of 200 kV.

X-ray photoelectron spectroscopy (XPS) analysis also was performed on the B_4C coatings with a PHI 5000c ESCE system (Perkin-Elmer, Wellesley, MA).

The coating was sectioned with a low-speed saw, was epoxy mounted, and was fine-polished using a No. 2000 SiC paper and 3, 1, and 0.25, diamond suspensions to minimize the smearing and pullout of particles. The cross-sectional microhardness was measured with Vickers hardness tester with a 300g load. An average microhardness of 10 points was the final result. Two techniques of porosity measurement were used, mercury intrusion porosimetry (MIP) and image analysis (IA) on cross-section by optical microscopy.

3. Results and Discussion

3.1 SEM Analysis

Observation of the fracture surface of the coating indicates several types of different structures. As shown in Fig. 1(a), the fracture surface is smooth and dense, and it exhibits a structure that is similar to a polished surface. Figure 1(a) indicates that the molten particles have spread significantly and that the contact between layers is coherent. This is the major structure in the as-sprayed coating. The other morphology is the observed lamellar packing, as shown in Fig. 1(b) where the contact between layers can be described as poor. The energy dispersive spectrum (EDS) results at 10 locations within Fig. 1(b) reveal only carbon. The results indicate that in this area, although representing only a small region in the as-sprayed coating, it is composed of the carbon phase.

Figure 2 shows a typical cross-section structure of the as-sprayed boron carbide coating. The layered splat structure is not distinct, but it was ascertained that the splats are from 5 to 10 μm thick at their centers and 50 to 80 μm long. There are several

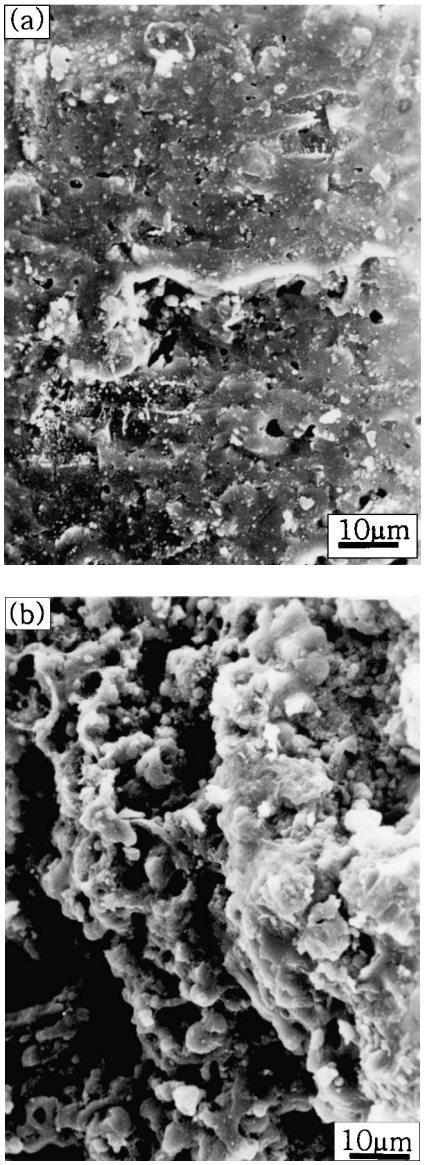

Fig. 1 Fracture morphologies of boron carbide coating

open interfaces between splats and some internal porosity within several splats. The number and size of the internal pores are greater than those at the interface. Some cracks running through the splats may also be seen. No original boron carbide powder agglomerates were observed, which indicated that the powders were well melted during the plasma spray process.

3.2 Phase Analysis

An important question related to maintaining the properties of a plasma-sprayed material is whether its phase purity is retained after plasma spraying. In the case of boron carbide, the XRD patterns of the powder and also of the sprayed coating are recorded in Fig. 3. It can be observed that no new phase is presented in the coating. However, the relative diffraction intensity of the carbon phase in the coating has become higher than that in the powder.

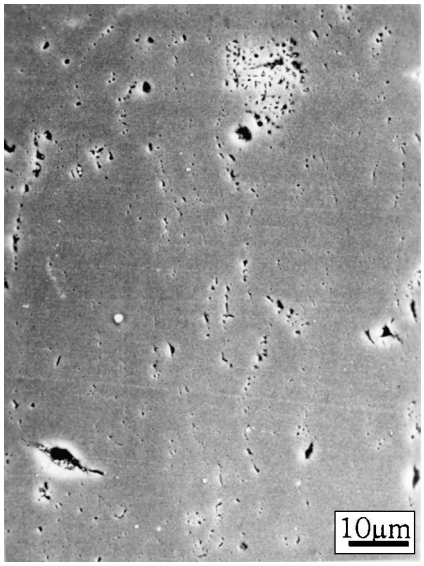

Fig. 2 Morphology of the polished cross-section of the boron carbide coating

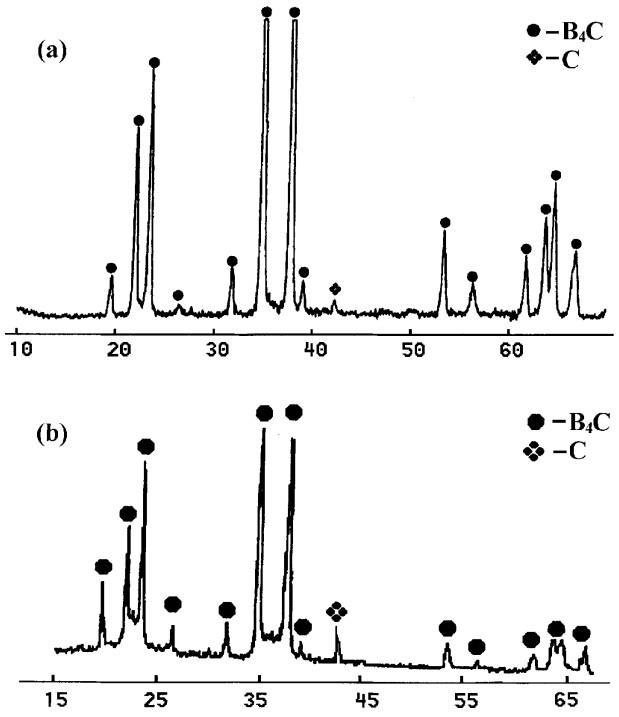

Fig. 3 The XRD patterns of boron carbide **(a)** powder and **(b)** coating

As shown in Fig. 4, the B_{1s} peak of the XPS spectrum of an as-sprayed coating could be deconvoluted into three components. A major part of boron is present as B_4C. The higher binding energy B_{1s} peaks at 190.3 eV, and 192.3 eV can be assigned to the low-valance B_xC

The phase composition change may be the contribution of B_4C powder decomposition during the plasma process. It could

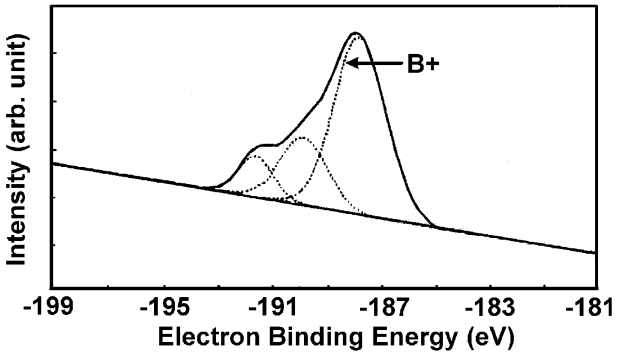

Fig. 4 XPS spectrum of the as-sprayed boron carbide coating

Table 1 The Properties of As-Sprayed Boron Carbide Coating (a)

	Porosity, %		
Coating	**IA**	**MIP**	**Microhardness, GPa**
B_4C coating	4.3	7.5	29

(a) IA—image analysis.

be inferred that B_4C powder would undergo the following reaction during the plasma process.

$$xB_4C \rightarrow 4B_xC + (x\text{-}4)C$$

and this is confirmed by TEM analysis (see Section 3.4). The carbon phase is difficult to melt during the plasma spray process and possibly is responsible for the poor structure observed in Fig. 1(b). No XRD data for the B_xC phase exists, therefore it is difficult to identify it by x-ray.

3.3 Mechanical Properties

Microhardness measurements test the coating's ability to resist penetration, which is based on the porosity content and overall structural integrity of the coating. Microhardness values, therefore, indicate the intersplat strength within the coating structure and, as well, are reflective of the phase present. Hardness data are reported in Table 1. The as-sprayed boron carbide coating has a microhardness of 29 GPa, which may be one of the highest values among plasma-sprayed coatings. It is considerably harder than the 1.2 to 2.1 GPa of plasma spray boron carbide coatings reported by Mallener et al.[3]

The distribution of hardness values, from 13 to 33 GPa, reflects the presence of the carbon phase in the coating. The existence of carbon and pores decreases the microhardness of the boron carbide coating compared to that of bulk materials (i.e., up to 49 GPa).

A low porosity is required to achieve high resistance to wear. The measurement of the porosity level by optical microscopy shows that the as-sprayed coating has an average porosity of 4.3%. However, the MIP result (Fig. 5) shows that its porosity is 7.5%, which is higher than that by optical microscopy. Results measured by MIP show that the average pore size is about 0.68 μm, which is consistent with the observation results with SEM. But there exist some large pores (i.e., >10 μm), which indicates that the measurement of MIP is more accurate for the as-sprayed

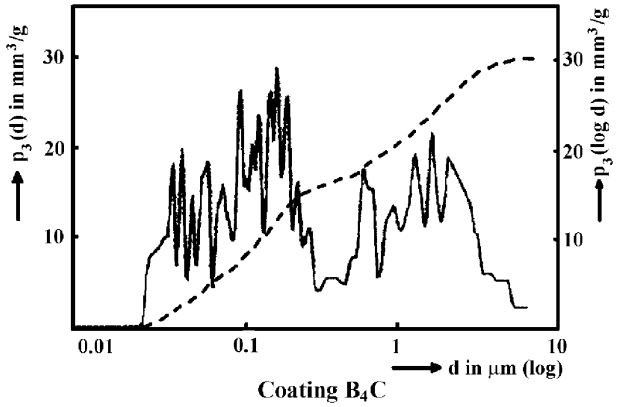

Fig. 5 The porosity and pore distribution of the boron carbide coating

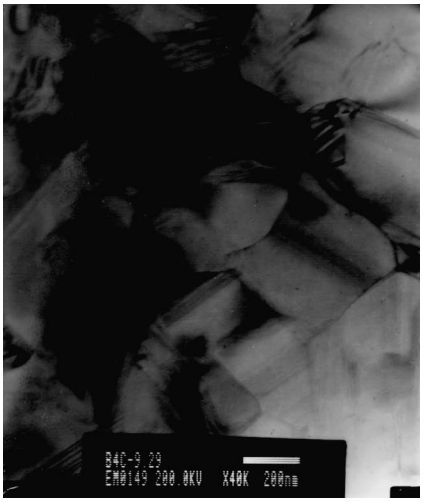

Fig. 6 TEM micrograph of the equiaxed grain in the boron carbide coating

coating because the loose carbon phase produces only a small quantity. This is difficult to ascertain by optical microscopy.

In the previous work,[2,3] the difficulty in spraying a B_4C coating lies in its oxidation and unmelting. In the present work, it has been found that if these two factors are overcome, the coating will be much denser. But the decomposition of the B_4C powder also would affect the microhardness and porosity of the boron carbide coating.

3.4 TEM Observation

Because the splat structure of the as-sprayed coating is not clear (as shown in Fig. 2), the internal columnar substructure cannot be observed, as has been reported by other investigations of normal plasma-sprayed coatings.[7] The most frequently observed structure in TEM examinations of as-sprayed coatings is equiaxed grains (Fig. 6). The size of grains is between 100 and 400 nm. The contact between these equiaxed grains is dense. The differing contrast between neighboring grains indicates that they have different crystallographic orientations. This was confirmed by selected area electron diffraction (SAED). The stress string could be observed in the equiaxed grain. It indicates that

there stress exists in the coating because of a mismatch between the boron carbide and the substrate.

Besides the equiaxed grains, there are twin structures in the coating. EDS analysis results indicated that area A in Fig. 7 consists of B and C elements, but the neighboring area B consists purely of the C element. The high-resolution transmission electron microscopy (HRTEM) is used to examine the area A in Fig. 7. The HRTEM image as shown in Fig. 8 indicates that there are four d values. Apparently, the d value 2.113 Å corresponds to the B_4C phase, while the other three d values correspond to the B_xC phase. This is confirmed by the phase analysis. From the above observation results, it could be inferred that the B_4C phase was partially decomposed into the B_xC and the carbon during the plasma-spraying process. The existence of B_xC and carbon phases would result in the inhomogeneity of an as-sprayed coating structure and would cause an increase of porosity and a decrease in the microhardness of the as-sprayed coating.

Two kinds of pores are present in the coating (Fig. 9). Lenticular pores along the grain boundary are due to loose contact between layers, and its size is about 100 to 200 nm. The spherical pores, which result from air trapping during the plasma-spraying process, are interlamellar. They are much larger than the lenticular pores. This agrees with the results observed by SEM.

In the conjunction of the splat area, amorphousness also is observed (Fig. 10), creating diffuse rings in the SAED pattern.

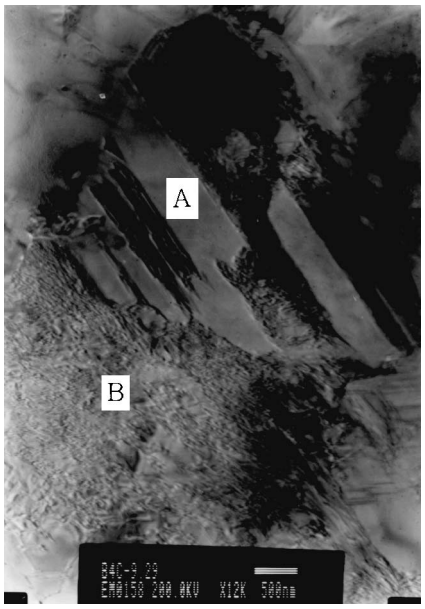

Fig. 7 TEM micrograph of the twin structure of the boron carbide coating

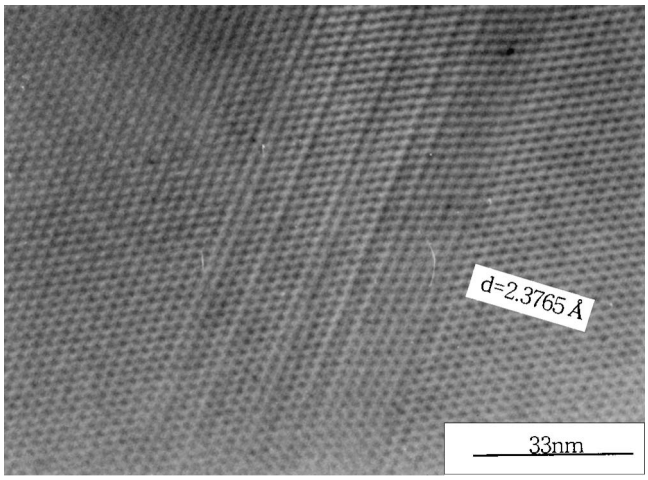

Fig. 8 The HRTEM image in area A in Fig. 7

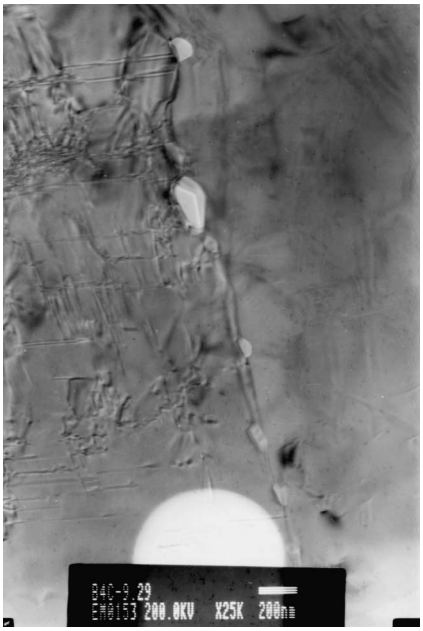

Fig. 9 The pores in the boron carbide coating

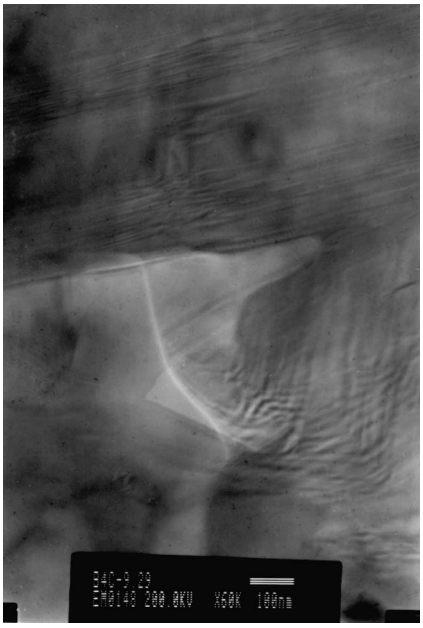

Fig. 10 The amorphous phase in the boron carbide coating

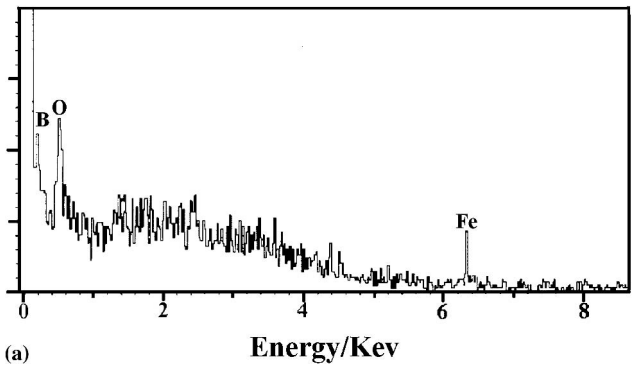

(a)

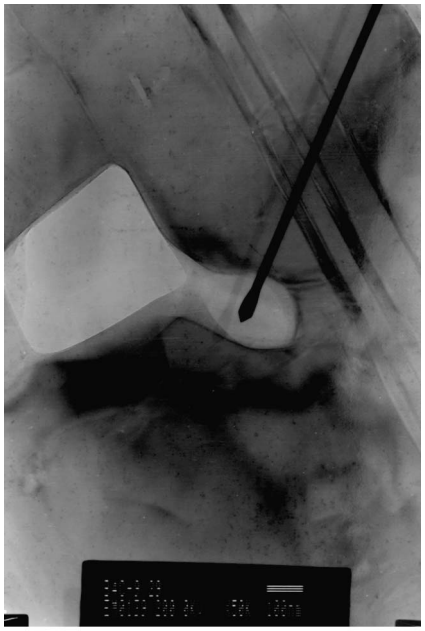

(b)

Fig. 11 EDS analysis and TEM micrograph of the impurity phase of the boron carbide coating

Clearly, it corresponds to the deposition of molten materials on a relatively cold surface and, therefore, to the most rapid rate of cooling, which leads to the suppression of nucleation.

Besides B_xC, B_4C, and carbon, other impurity phases exist (Fig. 11). The EDS analysis shows that point A consists of B, O, and Fe elements (i.e., Fe_3BO_6) by comparing the lattice of selected area diffraction (SAD) patterns with that of the Joined Committee on Powder Diffraction Standards (JCPDS) card (Table 2). The formation of the Fe_3BO_6 phase may be the result of a reaction of B_4C and Fe impurities in the powder during the plasma process. Like the carbon phase, the Fe_3BO_6 impurity phase also has a much lower microhardness than the major phase. It would also contribute to the decrease of microhardness of an as-sprayed boron carbide coating.

Table 2 The Comparison of Lattice Distance Between the Impurity Phase in Boron Carbide Coating and Composition Consisting of B, O, and Fe Elements

	Lattice Distance/Á			
Impurity phase	2.95	2.70	1.60	1.47
Fe_3BO_6	2.96	2.68	1.57	1.44

4. Conclusion

The high microhardness and low porosity of the B_4C coating was manufactured by an atmospheric plasma-spraying process. The as-sprayed coating here contains one major structure that has been equiaxed. The amount and sizes of the pores in the coating are small. Other phases besides the B_4C phase exist. The decomposition of B_4C powder during the plasma-spraying process results in the formation of B_xC and the increase of the carbon phase. The loose carbon phase is the major reason for the lower microhardness compared to bulk B_4C materials. The Fe_3BO_6 impurity phase also contributes to the low microhardness.

References

1. P. Bianchil, A. Fresion, F. Crodillot, and D. Schirmann: "Plasma Sprayed Boron Carbide Coatings as First Wall Material for Laser Fusion Target Chamber," in *Thermal Spray: Meeting the Challenges of the 21st Century*, C. Coddet, ed., ASM International, Materials Park, OH, 1998, pp. 945-50.
2. A. Cavasin, T. Brzezinski, S. Grenier, M. Smagorinski, and P. Tsantrizos: "W and B_4C Coatings for Nuclear Fusion Reactors," in *Thermal Spray: Meeting the Challenges of the 21st Century*, C. Coddet, ed., ASM International, Materials Park, OH, 1998, pp. 957-61.
3. W. Mallener, H.J. Grob, and D. Stover: "Properties of Plasma Sprayed Boron Carbide Coatings," in *Thermal Spray: Meeting the Challenges of the 21st Century*, C. Coddet, ed,. ASM International, Materials Park, OH, 1998, pp. 627-32.
4. M. Ducos and E. Gauthier: "Plasma Sprayed B_4C Coatings in Controlled Fusion Rectors," *Surface Eng.,* 1993, *9*(2), pp.127-30.
5. D. Schneider, T. Schwarz, and B. Schultrich: "Determination of Elastic Modulus and Thickness of Surface Layers by Ultrasonic Surface Waves," *Thin Solid Films,* 1992, *13*, pp. 219-23.
6. D. Morell: *Handbook of Properties of Technical & Engineering Ceramics*, Part 1, Kluwer Academic Publisher, London, 1963, p. 423.
7. R. Antonio, A.R.D. Arellano-Lopez, and K.T. Faber: "Microstrucutural Characterization of Small-Particle Plasma Spray Coatings" *J. Am. Ceram. Soc.,* 1999, *82*(8), pp. 2204-06.